Journal of Physics B:
Atomic, Molecular and
Optical Physics

PAPER

Periodic evolution of the Pearcey–Gaussian beam in the fractional Schrödinger equation under Gaussian potential

To cite this article: Ru Gao *et al* 2022 *J. Phys. B: At. Mol. Opt. Phys.* **55** 095401

IOP Publishing Journal of Physics B: Atomic, Molecular and Optical Physics
J. Phys. B: At. Mol. Opt. Phys. **55** (2022) 095401 (8pp) https://doi.org/10.1088/1361-6455/ac6554

Periodic evolution of the Pearcey–Gaussian beam in the fractional Schrödinger equation under Gaussian potential

Ru Gao, Teng Guo, Shumin Ren, Pengxiang Wang and Yan Xiao*

College of Physics and Electronics Engineering, Shanxi University, Taiyuan 030006, People's Republic of China

E-mail: xiaoyan@sxu.edu.cn

Received 8 January 2022, revised 1 April 2022
Accepted for publication 6 April 2022
Published 29 April 2022

Abstract

The dynamics of a Pearcey–Gaussian (PG) beam with Gaussian potential in the fractional Schrödinger equation (FSE) are investigated. In free space, varying the Lévy index offers a convenient way to control the splitting and bending angle of the beam. In the presence of Gaussian potential, with increasing propagation distance, the process is repeated in a breath-like motion. The periodicity also can be changed by adjusting the potential parameter and incident beam arguments, such as potential height, potential width and transverse wavenumber. The transmission and reflection of the beam can also be controlled by varying the potential parameters. Moreover, when a symmetrical Gaussian potential barrier is selected, total reflection is more likely to occur. These unique characteristics demonstrate the possibility of controlling the dynamics of PG beams with the FSE system.

Keywords: Pearcey–Gaussian beam, Fractional Schrödinger equation, Gaussian potential

(Some figures may appear in colour only in the online journal)

1. Introduction

In the past few decades, novel beams have attracted extensive attention as a mean of manipulating light in the related physical fields. Beams are described by particular functions, such as the Airy beam [1–4], Bessel beam [5], Gaussian beam [6] and Pearcey beam [7, 8], which are quite popular in the research of paraxial beam propagation in conventional optics. Scholars have focused more on the unique characteristics of the beam that can serve to apply in particle manipulation [9], microscopy and light bullets [10–12].

The Pearcey beam was proposed firstly in 1946 when Pearcey designed the structure of an electromagnetic field near caustic with the Pearcey function. The Pearcey function described the diffraction about a cusp of a caustic within the catastrophe the theory framework [13]. In 2012, Ring *et al* discovered theoretically that the Pearcey beam had these remarkable propagation properties: form-invariance, self-healing and spontaneous-focusing property [14]. Subsequently, a virtual source was presented to generate the Pearcey beam in 2014 [15]. In 2015, Kovalev *et al* regarded the Pearcey beam as a superposition of two first order half-Pearcey beams [16]. Inspired by these studies, a family of extended researches about Pearcey beam had been put forward [17–19], the majority of them focused on their features, such as one-dimensional finite energy Pearcey beam was investigated and revealed a dual self-accelerating behavior [20]. Then, the dynamics of partially coherent Pearcey–Gaussian (PG) beam propagating in the free space were discussed [21]. In 2021, a unique form of the odd PG beam under a parabolic potential was presented [22]. In the same year, dual-focusing property of a one-dimensional quadratically chirped PG beam was studied analytically and numerically [23]. Researchers have also analyzed other type of Pearcey beam theoretically and experimentally, including odd-Pearcey beam [24], Pearcey solitons [25], symmetric PG beam [26–28] and PG vortex beam [29, 30].

* Author to whom any correspondence should be addressed.

On the other hand, the fractional effect, such as quantum oscillator and Talbot effect, widely existed in various fields of quantum mechanics. In 2000, the fractional Schrödinger equation (FSE), a generalization of the standard Schrödinger equation, first formulated by Laskin [31–33], had received significant attention. Soon afterwards, an experimental structure of the FSE was designed by Longhi [34], the model based on transverse light dynamics in aspherical optical cavities. This scheme sparked a growing interest to explore the dynamics of beam in the FSE. Up to the present, FSE had been comprehensively discussed in but not confined to party-time-symmetry [35], gap solitons [36] and dynamics of Airy beam [37, 38]. In 2015, the dynamics of beam in the FSE was probed and discovered that it follows a zigzag and funnel-like trajectory in real space on one or two dimensions [39]. Among the investigations, the dynamics of the Gaussian beam with a variable coefficient had been reported and the results have shown that the beam splits into two sub-beams [40], meanwhile, they exhibited a periodically oscillating behavior in the absence of the chirp, while there is chirp, one of the splitting beams was suppressed, and another shown a periodic oscillation. By adjusting the double-barrier potential, it can also easily achieve the beam propagation management [41, 42]. With the deepening research for the FSE, more results have been observed, such as the evolution of Airy beams in a linear potential [43], dynamics of Bessel–Gaussian beam [44], propagation of Airy–Gaussian beam with Gaussian potential [45, 46] and so on. In addition, the evolution of super-Gaussian beam under the FSE has been considered numerically and theoretically [47]. Recently, much interest has also been drawn to Airy–Gaussian vortex beams and abruptly autofocusing circular Airy–Gaussian vortex beams, modeled by the FSE [48, 49], which have extremely reference value to the study of FSE.

Similar to the Bessel beam and Airy beam, a pure Pearcey beam can become finite and physically accomplished by modulating the Pearcey beam with a Gaussian function in real space, whose acceleration property could be completely realized in theory and experiment. At the same time, the purpose of controlling the beam can be achieved by adjusting the potential parameters. Therefore, it is essential to investigate the dynamics of the PG beam with a Gaussian potential in the framework of FSE.

In this letter, the dynamics of a PG beam with a Gaussian potential based on the FSE by using the split-step Fourier method are investigated. In the absence of Gaussian potential, the beam splitting, and its bending degree is controlled by the Lévy index. Furthermore, the beam exhibits a periodic evolution in the Gaussian potential. Under a certain circumstance, light beam may even transmit and reflect. The above conclusion provides a powerful and effective way for the beam control and can find many applications in optics, such as light switch and optical router.

2. Propagation model

In the paraxial approximation, spatial beam evolving along direction z is governed by such a FSE which can be described in the normalized form.

$$i\frac{\partial}{\partial z}\psi(x,z)-\frac{1}{2}\left(-\frac{\partial^2}{\partial x^2}\right)^{\frac{\alpha}{2}}\psi(x,z)=V(x)\psi(x,z), \quad (1)$$

where $\psi(x,z)$ is the field amplitude of optical beam, the dimensionless transverse coordinates and propagation distance are denoted by x and z, respectively. $x=\eta/x_0$ and $z=\xi/kx_0{}^2$, we note here that x_0 is the transverse scale, kx_0^2 is the corresponding Rayleigh range. $k=2\pi n/\lambda_0$ stands for the wavenumber, n is the photorefractive index, α represents Lévy index and λ_0 is the wavelength. When the Lévy index takes 2, FSE becomes into a standard Schrödinger equation. Firstly, the external potential is not considered. By using the Fourier transform method, we can obtain the following equation:

$$i\frac{\partial}{\partial z}\hat{\psi}(k,z)-\frac{1}{2}|k|^{\alpha}\hat{\psi}(k,z)=0, \quad (2)$$

in equation (2), $\hat{\psi}(k,z)=\int_{-\infty}^{+\infty}\psi(x,z)\exp(-ikx)dx$ is the Fourier transform of $\psi(x,z)$ and k denotes the spatial frequency. The solution of equation (1) with initial condition $\psi(x,0)$ can be written by

$$\psi(x,z)=\frac{1}{2\pi}\int_{-\infty}^{+\infty}\hat{\psi}(k,0)\exp\left(-i\frac{1}{2}|k|^{\alpha}z\right)e^{ikx}\,dk. \quad (3)$$

Herein, a PG beam as an input is considered as:

$$\psi(x,0)=A_0Pe(x)\exp(-\chi_0{}^2x^2)\exp(-i\mu x), \quad (4)$$

in which μ express a transverse wavenumber, χ_0 is the distribution factor, A_0 is the amplitude and $Pe(x)=\int_{-\infty}^{+\infty}\exp\left[i\left(s^4+sx\right)\right]ds$ represents the Pearcey function.

To realize the propagation control of the PG beam, we consider a Gaussian potential, which has the following form:

$$V(x)=p\left\{C_1\exp\left[-\frac{(x-x_0)^2}{d_0{}^2}\right]+C_2\exp\left[-\frac{(x+x_0)^2}{d_0{}^2}\right]\right\}, \quad (5)$$

where p is the potential height, x_0 denotes the central location of the potential, d_0 stands for the potential width. In addition, when C_1 and C_2 are positive, it represents the potential barrier, conversely, when their sign is negative, it corresponds to the potential well.

3. Results and discussion

3.1. Propagation dynamics of Pearcey beam without the Gaussian potential

Now, we analyze the propagation of the Pearcey beam without the Gaussian potential in the free space by using the split-step Fourier method.

In the following studies, we show the propagation property of Pearcey beam with different Lévy index without the Gaussian potential in figure 1. As can be seen from figure 1, the Pearcey beam splits into two sub-beams accelerating in opposite directions after a short focusing, and exhibits a dual self-bending behavior. During the propagation, these sub-beams are symmetric about $x=0$. In addition, from

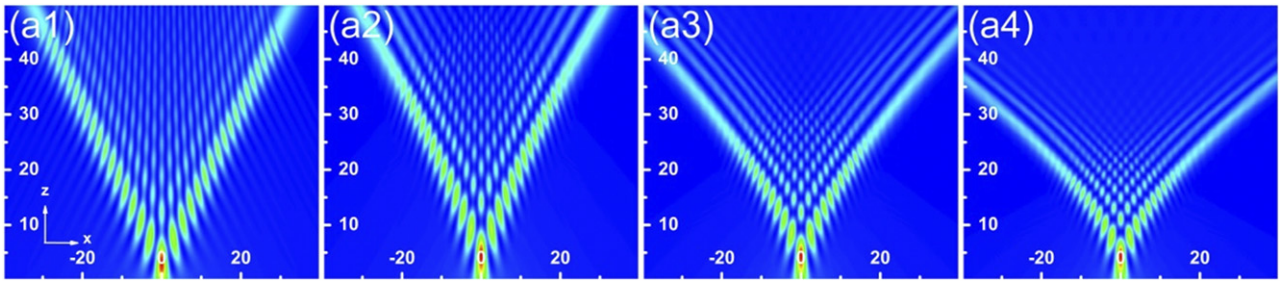

Figure 1. Evolution of the Pearcey beam without the Gaussian potential barriers under different Lévy index α: (a1) $\alpha = 1$ (a2) $\alpha = 1.5$ (a3) $\alpha = 1.8$ (a4) $\alpha = 2$. The other parameters are $\chi_0 = 0.01$, $\mu = 0$.

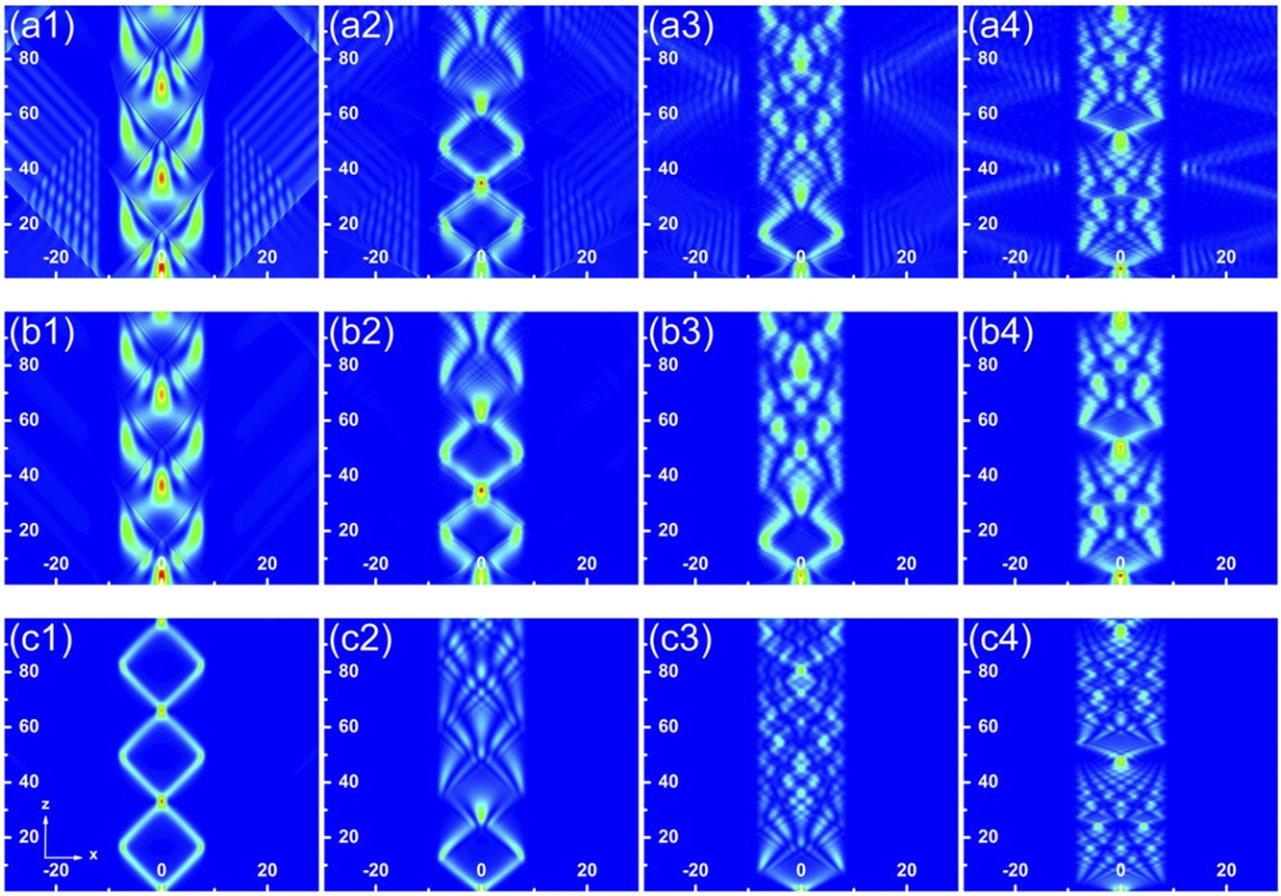

Figure 2. The evolution plots of the PG beam with Gaussian potential barriers. Here, $\chi_0 = 0.01, 0.1, 0.9$ from top row to bottom row, and $\alpha = 1, 1.2, 1.5, 2$ from left column to right column, respectively. The other parameters are $x_0 = 10$, $p = 20$, $d_0 = 1$.

figures 1(a1)–(a4), one can substantially find interference pattern in the middle of the sub-beams, which is similar to fish scales. As the Lévy index increases, region of interference pattern gradually decreases, moreover, the profile of the sub-beam changes from straight line to curved, and the degree of bending also increases. For Lévy index $\alpha = 2$ in figure 1(a4), the curvature of the main lobe reaches its maximum. This property is remarkably different from the case in the FSE. The Lévy index, thus, can be utilized to control the degree of bending of the beam.

3.2. Evolution properties of PG beam with the Gaussian potential

Here we focus on the dynamics of PG beam with the Gaussian potential, the potential is introduced to control the propagation properties of PG beam modeled by the FSE, some of the original properties have been discussed.

We consider the evolution of PG beam in the Gaussian potential under different Lévy index α and distribution factor χ_0 in figure 2, χ_0 determines whether the incident beam tends to be Pearcey or Gaussian distribution. As seen in

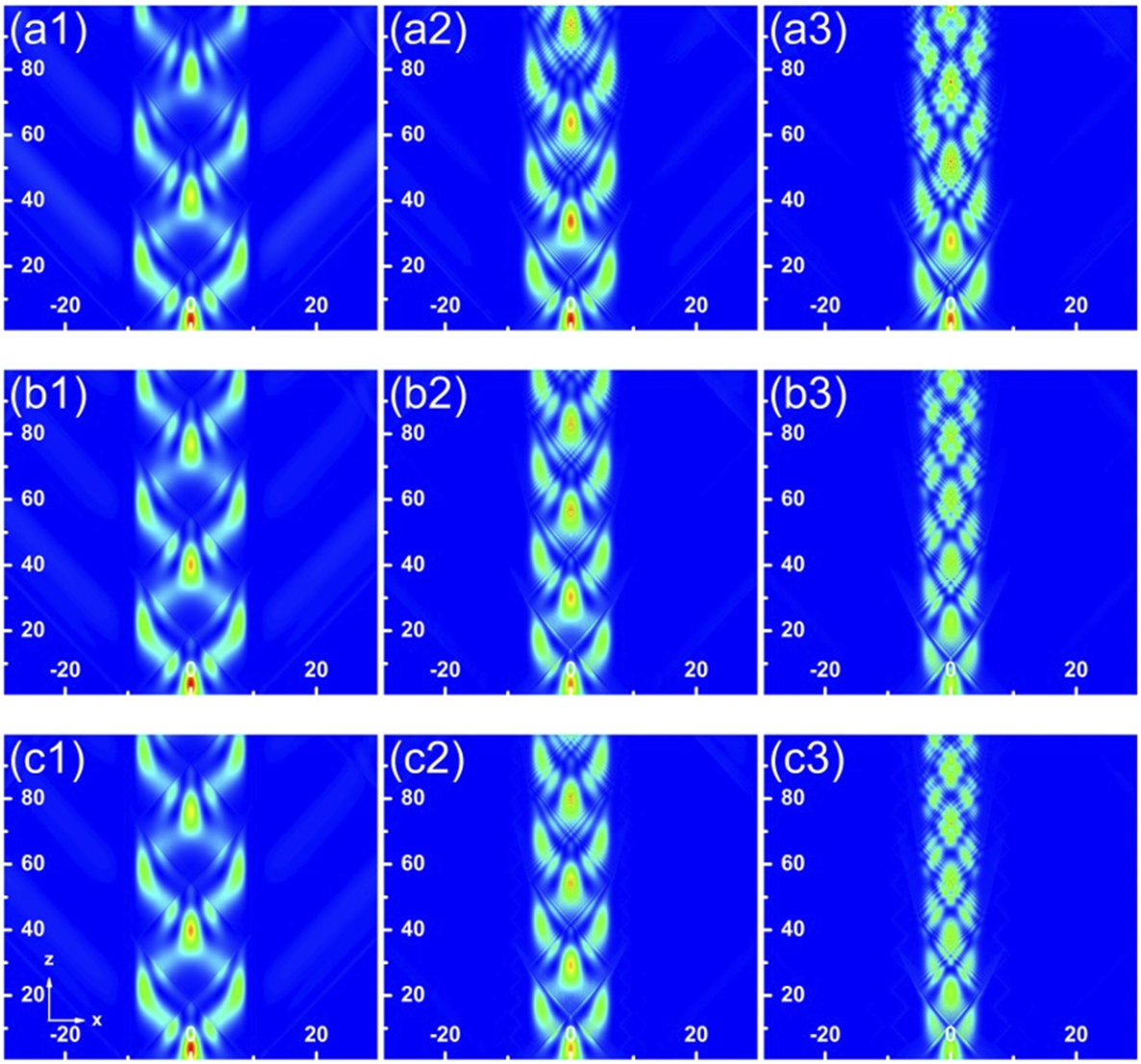

Figure 3. The evolution of the PG beam with Gaussian potential barriers for different potential width d_0 and potential height p. The potential height is respectively $d_0 = 0.5, 1.6, 2.4$ from left column to right column. The potential width is $p = 5, 45, 100$ from top to bottom. Here, the other parameters are the same as figure 1.

figure 2, on the whole, the incident beam splits into two sub-beams after a short distance and then alters the transmission direction after being reflected by the potential barrier, the repetition of this process results in periodic self-imaging properties. Although the sub-beam is well localized in the potential barriers, it is evident to recognize that apparent transmission phenomenon occurs in figures 2(a1)–(a4). This is due to the leakage of the side lobe at large incident beam. On the other hand, characteristics of the Gaussian beam dominate with the gradually increasing of χ_0. Remarkably, the side lobe of PG beam in figures 2(c1)–(c4) decreases sharply, the intensity distribution still shows periodic evolution, and it is the most distinct in figure 2(c1). With the increase of α, the beam ultimately evolves into chaos and the speed of formation is getting faster. The explanation of this phenomenon is that the periodic transmission of the beam, wherein with the increasing of Lévy index, the interference of the reflected beams becomes stronger, it is the existence of simultaneous interaction and interference force of reflected beams that lead to the chaotic behavior of PG beam propagating in potential barriers.

Next we analyze the characteristics of PG beam in Gaussian potential barriers with different potential height p and potential width d_0, the corresponding results are shown in figure 3. The diffraction effect of the PG beam and the Gaussian potential barrier both result in that the light beam exhibits in a periodically bound state. In figure 3, much as in the pioneering studies, the intensity distribution of the PG beam is characterized by periodic evolution within a certain region. Our results indicate that with the increasing of p, the transverse region of the beam bound state becomes narrower and that the period gradually reduces in figures 3(a2)–(c2) and (a3)–(c3). When the potential width is small, this phenomenon is not obvious, only partial transmission occurs (see figures 3(a1)–(c1)). The mechanism by which potential height affects the period can be explained in this way: the potential barrier seems to be a bulge with an ideal reflection wall, in which the light beam transmits but hardly

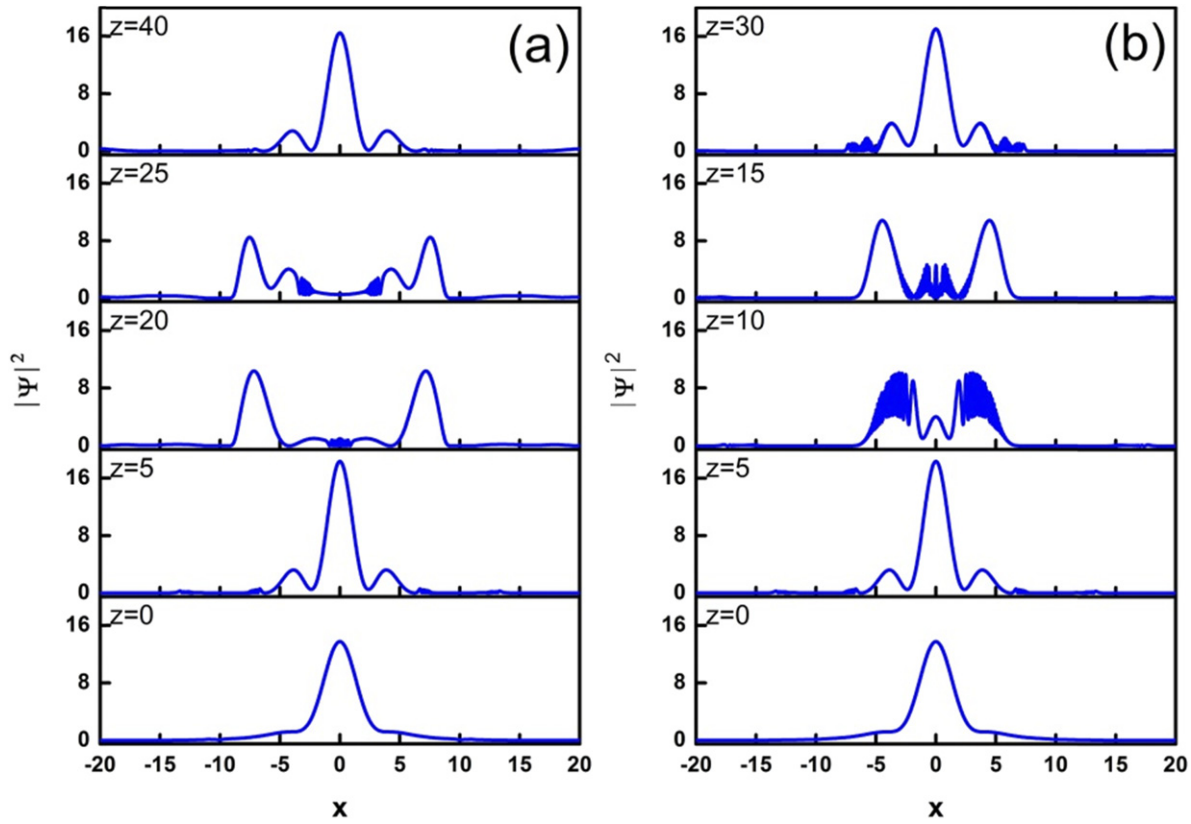

Figure 4. The intensity distribution of PG beam with Gaussian potential barriers at different potential width d_0. (a) $d_0 = 0.6$ (b) $d_0 = 1.8$. Here, the other parameters are $\chi_0 = 0.1$, $\mu = 0$, $\alpha = 1.3$, $x_0 = 10$, $d_0 = 2$.

passes through the wall. If the potential barrier is high enough, its shape will change, the bound space of the potential barrier will become smaller, which affecting the reflection position of the beam, and leads to the decrease of propagation periodicity. Similarly, as d_0 increases, these behaviors are consistent with the increasing of p. Furthermore, the larger potential width, the more the inner wall of the potential barrier expands inward. As a result, the bound space and the period of the beam become smaller, displayed in figures 3(a1)–(a3). These phenomena can be employed in optical tweezers and optical traps.

To better understand the above phenomenon, figure 4 depicts the intensity distribution of the PG beam under different potential width d_0. In figure 4(a), it is clearly evident that the intensity distribution of the sub-beams are always symmetric about $x = 0$. As the rising of the transmission distance, PG beam exhibits a periodic evolution. Extremely when $z = 0$, a peak is formed. However, these behaviors change dramatically for the cases with the increasing of z, in which the beam starts to split and the side lobe begins to appear, at the same time, the energy of the main lobe becomes decrease when in the middle of a period. Whereas when the transmission distance is large enough, the energy of the side lobe turns weaker and converges towards the main lobe, which regains its dominance. The whole process presents a periodic evolution. There is a similar phenomenon in figure 4(b). The comparison of (a) and (b) in figure 4 discover that the distance required to complete a period for $d_0 = 1.8$ is shorter than that $d_0 = 0.6$, and the more intense evolution of the beam at a large potential barrier width. The explanation for this phenomenon is that the increase in d_0 produces a thicker potential barrier wall, which allowing the beam to reflect in a narrow range. This leads to a smaller period. Previous studies have also shown that the PG beam exhibits a periodic stable bound state by regulating the parameter of the potential. This helps achieve the purpose of controlling the beam.

The intensity evolution of the PG beam under the Gaussian potential barriers with varying the central position of potential x_0 and transverse wavenumber μ is depicted in figure 5. We discover that the deflection direction and the deflection angle of the beam can be controlled by adjusting the μ. In addition, the PG beam shows the 'mirror reflection' phenomenon. It is also shown, when $\mu = 0$ that the incident beam splits into two sub-beams and undergoes the periodic evolution. While the sub-beam oscillates along the zigzag path and the symmetry disappear when $\mu \neq 0$. It is obvious that the initial input deflects to the right when $\mu < 0$, but situation is reversed when $\mu > 0$. Therefore, by varying the transverse wavenumber, the intriguing zigzag propagation may have potential applications in the light modulators and optical switch. As the value of $|\mu|$ increases, there is even a transmission phenomenon in figures 5(a1)–(c1) and (a5)–(c5), owing to a sufficient velocity, which causes the potential barrier wall is broken through by the incident beam, moreover, the amplitude of lateral swing and the period increase significantly with the growth of the

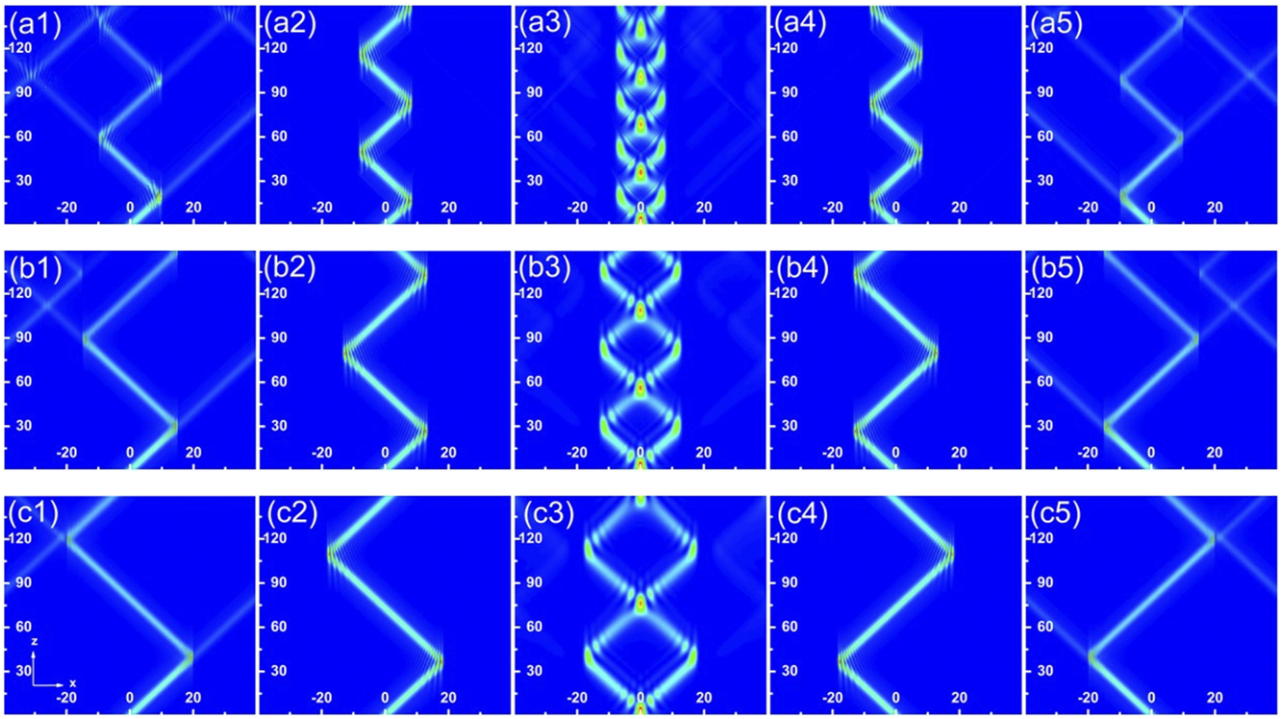

Figure 5. The evolution of the PG beam with the Gaussian potential barriers. Here, $x_0 = 10, 15, 20$ from top row to bottom row, and $\mu = -60, -3, 0, 3, 60$ from left column to right column, respectively. The other parameters are $\chi_0 = 0.1$, $d_0 = 1$, $p = 30$, $\alpha = 1$.

location of the potential barrier. As a result, the confinement space of the beam can be changed by adjusting the x_0.

To realize the propagation control of light beam, we consider the evolution of the PG beam with different combination of potential wells and barriers in figure 6. When in the double potential wells, the beam splits first, a small portion of sub-beam is reflected by the barrier wall, and most of it is transmitted, which generate the interference pattern in the middle region of two potential wells (see figures 6(a1)–(c1)). Similarly, under a single potential well, the split beam propagates to the left and hits the potential well, both transmission and reflection occur simultaneously, but most of the beam is transmitted and only a fraction is reflected (see figures 6(a2)–(c2)). In addition, under the symmetric potential barriers, the two sub-waves are reflected and then converge again after hitting the potential barrier wall, forming a parallelogram transmission pattern, and this process carries on periodic evolution (see figures 6(a3)–(c3)). In the same way, when the beam propagates in a single potential barrier, the left sub-beam meets the potential barrier wall, and only a small part is transmitted. The majority of the beam is reflected, and the reflected part on the left has the same transmission direction as the right sub-beam. The beam realizes basically non-diffraction transmission (see figures 6(a4)–(c4)). Furthermore, when the incident beam is transmitted in the mixture of a single well and a barrier (see figures 6(a5)–(c5)), most of the left beams achieve the transmission after encountering the potential well, while most of the right beams are reflected due to the effect of the potential barrier. Moreover, we note from the illustrations that when the beam tends to Pearcey distribution (see figures 6(a1)–(a5)), there are many side lobes around the main lobe to participate in the movement, but when the incident beam gradually tends to the Gaussian distribution, the side lobe is significantly reduced, and the effective width is narrower than that of Pearcey beam (see figures 6(c1)–(c5)), which means that the beam width is affected by the side lobe. It is also found that when the beam propagates in the potential barrier, most of it is reflected and only a little portion is transmitted, while when it travels in a well, the situation is just the opposite. In other words, the ability of the total reflection of the potential barrier is stronger. One important needs to be pointed out that this result also suits for the case of optical control.

The reflectivity R of the beam as well as the corresponding transmissivity T with the variation of potential height p and the potential width d_0 are displayed in figures 7(a) and (b), separately. From figure 7(a), we qualitatively observe that with the continuous increasing of potential height, the reflectivity increases rapidly, and approaches to a stable value, it closes to 1. But the transmissivity drops dramatically and eventually tends towards 0. It also can be seen from figure (a) that the curve changes most obviously in the range of p from 0–5, and when $p > 5$, the changes of R and T tend to be gentle. Another major notable point is that the reflectance and transmittance always obey the propagation law: $T = 1 - R$. From figure 7(b), we derive the change is most pronounced when d_0 is less than 0.5. Additionally, the transformation rate of figure (b) is similar to that of figure (a). By varying the potential barrier parameters, one can easily obtain the transmissivity and reflectivity of the beam.

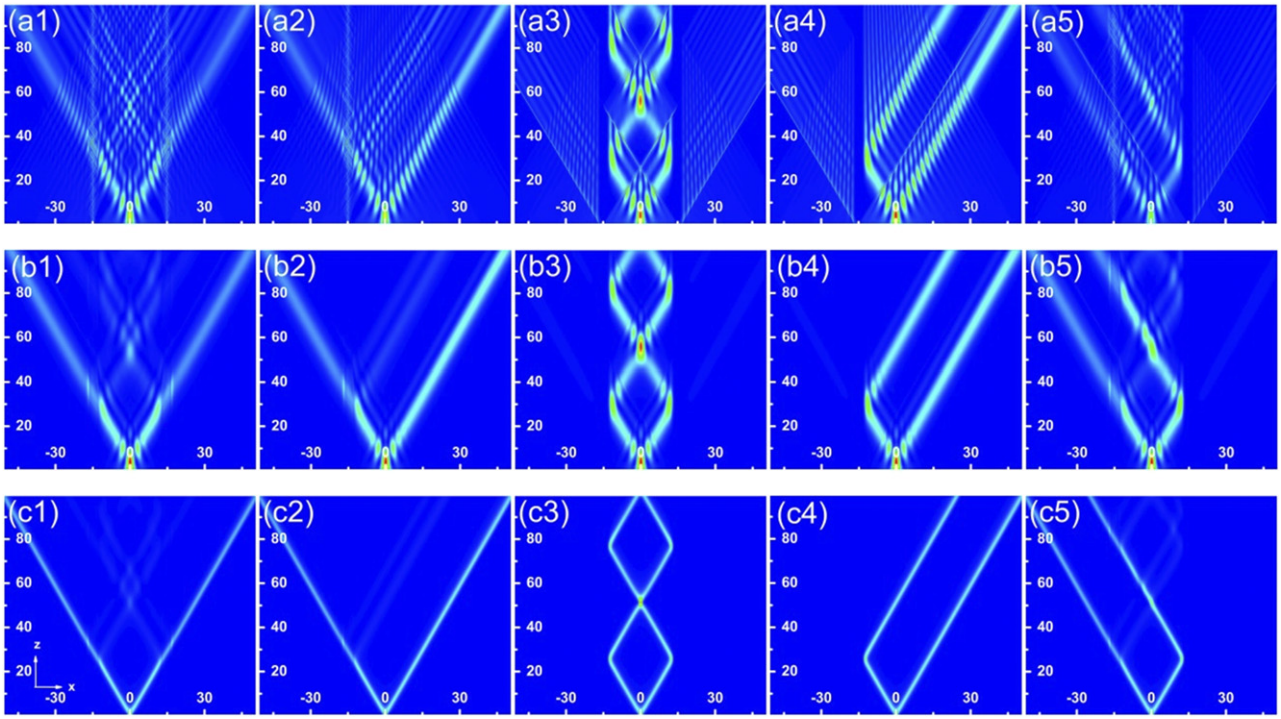

Figure 6. The evolution of the PG beam under the combination of potential wells and barriers. Here, $\chi_0 = 0.01, 0.1, 1$ from top row to bottom row. Symmetric double wells, a single well, symmetric double barriers, a single barrier, the combination of a single well and a single barrier from left column to right column. The other parameters are $\mu = 0$, $p = 30$, $x_0 = 15$, $d_0 = 1$, $\alpha = 1.02$.

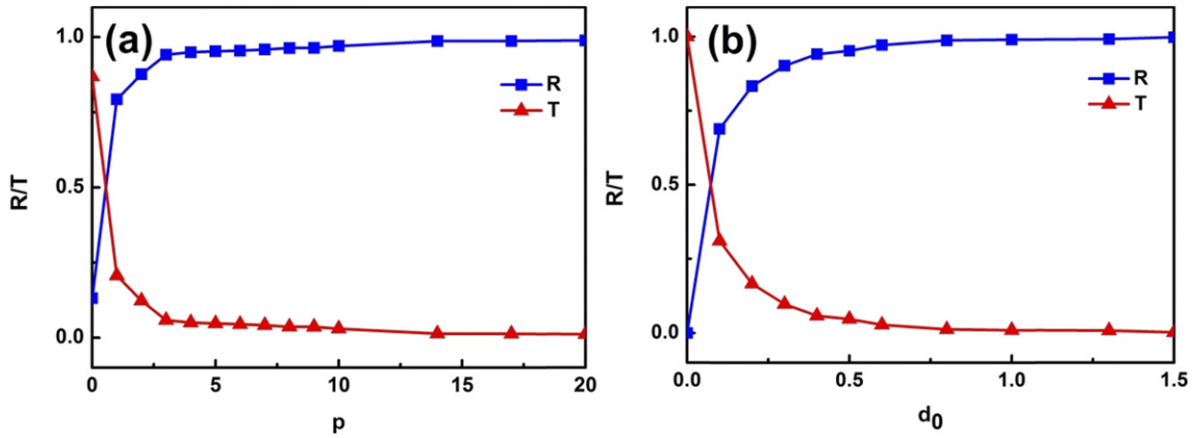

Figure 7. The reflectivity R and the transmissivity T varying with the potential barrier parameters. (a) Potential height; (b) potential width. The other parameters are $\mu = 0$, $\chi_0 = 0.1$, $\alpha = 1$, $x_0 = 10$, $d_0 = 1$.

4. Conclusion

In this work, the propagation dynamics of the PG beam with the Gaussian potential by utilizing the split-step Fourier method are demonstrated, based on the FSE in the paraxial approximation. In the free space, the PG beam evolves into two sub-beams, whose bending angle is affected by the Lévy index. However, it should be noted that the PG beam exhibits periodic evolution under the Gaussian potential, and it can be changed by adjusting the suitable potential parameters, exemplarily, potential height and the potential width. Furthermore, the distribution factor is also an essential influencing element. When it tends to 0, the beam shows the characteristics of the Pearcey. In contrast, when it approaches 1, the properties of the Gaussian beam will dominate. Chaos can also appear as the Lévy index growing during the propagation. Subsequently, we probe the transverse wavenumber μ, which can affect the period and deflection direction of the PG beam. When $\mu = 0$, the PG beam has a similar cyclical evolution, except that, for $\mu > 0$ and $\mu < 0$, the sub-beams deflect in the opposite direction. These results pave the way to future optical switch and light routing. In addition, we discuss the transmission and reflection of the beam under different combination of the potential well and barrier, and discover that under the symmetrical barriers,

the beam is easier to achieve total reflection. Additionally, the transmission and reflection of the light beam follow a certain rule. We believe that our results not only enhance the research interest of FSE but also the fabrication of light modulators in the future.

Data availability statement

All data that support the findings of this study are included within the article (and any supplementary files).

ORCID iDs

Yan Xiao https://orcid.org/0000-0002-1943-9932

References

[1] Siviloglou G A and Christodoulides D N 2007 *Opt. Lett.* **32** 979–81
[2] Siviloglou G A, Broky J, Dogariu A and Christodoulides D N 2007 *Phys. Rev. Lett.* **99** 213901
[3] Siviloglou G A, Broky J, Dogariu A and Christodoulides D N 2008 *Opt. Lett.* **33** 207–9
[4] Broky J, Siviloglou G A, Dogariu A and Christodoulides D N 2008 *Opt. Express* **16** 12880–91
[5] McGloin D and Dholakia K 2005 *Contemp. Phys.* **46** 15–28
[6] Zhang Y, Zhong H, Belić M R, Ahmed N, Zhang Y and Xiao M 2016 *Sci. Rep.* **6** 23645
[7] Hu H, Xu C, Lin M and Deng D 2021 *Results Phys.* **26** 104416
[8] Ren Z, Ying C, Jin H and Chen B 2015 *J. Opt.* **17** 105608
[9] Grier D G 2003 *Nature* **424** 810–6
[10] Aleksanyan A, Kravets N and Brasselet E 2017 *Phys. Rev. Lett.* **118** 203902
[11] Yang Y, Zhao Q, Liu L, Liu Y, Rosales-Guzmán C and Qiu C-w 2019 *Phys. Rev. Appl.* **12** 064007
[12] Abdollahpour D, Suntsov S, Papazoglou D G and Tzortzakis S 2010 *Phys. Rev. Lett.* **105** 253901
[13] Pearcey T 1946 *London, Edinburgh Dublin Phil. Mag. J. Sci.* **37** 311–7
[14] Ring J D, Lindberg J, Mourka A, Mazilu M, Dholakia K and Dennis M R 2012 *Opt. Express* **20** 18955–66
[15] Deng D, Chen C, Zhao X, Chen B, Peng X and Zheng Y 2014 *Opt. Lett.* **39** 2703–6
[16] Kovalev A A, Kotlyar V V, Zaskanov S G and Porfirev A P 2015 *J. Opt.* **17** 035604
[17] Ren Z, Fan C, Shi Y and Chen B 2016 *J. Opt. Soc. Am.* A **33** 1523–30
[18] Sun C, Deng D, Yang X and Wang G 2020 *Opt. Express* **28** 325–33
[19] Chen X *et al* 2018 *Opt. Lett.* **43** 3626–9
[20] Zang F, Wang Y and Li L 2019 *Results Phys.* **15** 102656
[21] Zhou X, Pang Z and Zhao D 2020 *Opt. Lett.* **45** 5496–9
[22] Mo Z, Wu Y, Lin Z, Jiang J, Xu D, Huang H, Yang H and Deng D 2021 *Appl. Opt.* **60** 6730–5
[23] Zang F, Liu L, Deng F, Liu Y, Dong L and Shi Y 2021 *Opt. Express* **29** 26048–57
[24] Liu Y, Xu C, Lin Z, Wu Y, Wu Y, Wu L and Deng D 2020 *Opt. Lett.* **45** 2957–60
[25] Zannotti A, Rüschenbaum M and Denz C 2017 *J. Opt.* **19** 094001
[26] Wu Y *et al* 2021 *Opt. Lett.* **46** 2461–4
[27] Xu C, Wu J, Wu Y, Lin L, Zhang J and Deng D 2020 *Opt. Commun.* **464** 125478
[28] Chen R, Yi K, Peng Y, Zou B and Hong W 2020 *Results Phys.* **18** 103255
[29] Chen X, Deng D, Wang G, Yang X and Liu H 2019 *Opt. Lett.* **44** 955–8
[30] Lin Z, Wu Y, Qiu H, Fu X, Chen K and Deng D 2021 *Commun. Nonlinear Sci. Numer. Simul.* **94** 105557
[31] Laskin N 2000 *Phys. Rev.* E **62** 3135–45
[32] Laskin N 2000 *Phys. Lett.* A **268** 298–305
[33] Laskin N 2002 *Phys. Rev.* E **66** 056108
[34] Longhi S 2015 *Opt. Lett.* **40** 1117–20
[35] Zhang Y, Zhong H, Belić M R, Zhu Y, Zhong W, Zhang Y, Christodoulides D N and Xiao M 2016 *Laser Photonics Rev.* **10** 526–31
[36] Huang C and Dong L 2016 *Opt. Lett.* **41** 5636–9
[37] Huang X, Deng Z and Fu X 2017 *J. Opt. Soc. Am.* B **34** 976–82
[38] He S, Malomed B A, Mihalache D, Peng X, He Y and Deng D 2021 *Phys. Lett.* A **404** 127403
[39] Zhang Y, Liu X, Belić M R, Zhong W, Zhang Y and Xiao M 2015 *Phys. Rev. Lett.* **115** 180403
[40] Zang F, Wang Y and Li L 2018 *Opt. Express* **26** 23740–50
[41] Huang X, Shi X, Deng Z, Bai Y and Fu X 2017 *Opt. Express* **25** 32560–9
[42] Huang C and Dong L 2017 *Sci. Rep.* **7** 5442
[43] Chen W, Wang T, Wang J and Mu Y 2021 *Opt. Commun.* **496** 127136
[44] Zhang Y, Wu Z, Ru J, Wen F and Gu Y 2020 *J. Opt. Soc. Am.* B **37** 3414–21
[45] Xiao Y, Zhang J and Wang P 2021 *Optik* **235** 166627
[46] Xiao Y, Wang P, Zhang J, Guo T, Gao R and Ren S 2021 *Optik* **243** 167431
[47] Zhang L, Li C, Zhong H, Xu C, Lei D, Li Y and Fan D 2016 *Opt. Express* **24** 14406–18
[48] He S *et al* 2021 *J. Opt. Soc. Am.* B **38** 3230–6
[49] He S, Malomed B A, Mihalache D, Peng X, Yu X, He Y and Deng D 2021 *Chaos Solitons Fractals* **142** 110470